Polymer 51 (2010) 5556–5566

Contents lists available at ScienceDirect

Polymer

journal homepage: www.elsevier.com/locate/polymer

Effect of comonomer-unit composition and its distribution of bacterial poly(3-hydroxybutyrate-*co*-3-hydroxyhexanoate) on miscibility and physical properties of its blend with poly(ethylene oxide)

Fang Yu [a], Nobuo Nakamura [b], Yoshio Inoue [a,*]

[a] Department of Biomolecular Engineering, Tokyo Institute of Technology, Nagatsuta 4259-B-55, Midori-ku, Yokohama 226-8501, Japan
[b] GP Business Development Division, KANEKA Corporation, 5-1-1, Torikai-Nishi, Settsu, Osaka 566-0072, Japan

ARTICLE INFO

Article history:
Received 15 July 2010
Received in revised form
15 September 2010
Accepted 15 September 2010

Keywords:
Miscibility
Polymer blending
Polymer physics

ABSTRACT

In order to investigate the effect of comonomer-unit composition and its distribution of bacterial poly (3-hydroxybutyrate-*co*-3-hydroxyhexanoate) [P(3HB-*co*-3HHx)] on the miscibility of its blend with poly (ethylene oxide) (PEO), as-bacterially synthesized and well-fractionated P(3HB-*co*-3HHx)s with different 3HHx unit content were blended with PEO at different content. It is found that the miscibility between P (3HB-*co*-3HHx) and PEO decreases dramatically with increasing both 3HHx unit content of P(3HB-*co*-3HHx) and PEO content in the blend. The miscibility is also found to be significantly affected by the comonomer-unit compositional distribution of P(3HB-*co*-3HHx). Strongly depending on the comonomer-unit composition of P(3HB-*co*-3HHx) and PEO content in the blend, thermal stability and mechanical properties of P(3HB-*co*-3HHx) can be regulated by blending with PEO. Moreover, PEO exhibits good dispersion in P(3HB-*co*-3HHx) matrix. It is concluded that the P(3HB-*co*-3HHx)/PEO binary blend can exhibit diverse properties by varying the comonomer-unit composition and comonomer-unit compositional distribution of P(3HB-*co*-3HHx) as well as the PEO content in the blend.

1. Introduction

In the second half of last century, a production of certain materials has truly skyrocketed. They were synthetic polymers, also known as plastic, the majority of which are petroleum-derived. However, with the depletion of the global petroleum resource and increasing of solid waste which need hundreds and thousands years to degrade, plastics derived from new green energy are being researched all over the world. The emergence of biomass-derived polymers brings new hopes for solving these environmental problems, and accordingly they are being paid more and more attentions as one of the potential and perspective alternatives for petroleum-based polymers. The family of poly(hydroxyalkanoic acids) (PHAs) is one typical family of biomass-derived, biodegradable and biocompatible polymers, which can be produced by a wide variety of microorganisms and biodegradable under the actions of various microorganisms and/or enzymes [1–6]. In particular, the bacterially synthesized poly(3-hydroxybutyrate) [P(3HB)] [7], the most promising and attractive member of PHAs, has already been industrially commercialized and its applications have covered widely from agricultural and marine to medical field. However, there are still some issues concerning on the industrial processing of P(3HB), such as narrow processability window and low impact resistance, which confine greatly its industrial applications [8–10]. Studies on P(3HB) copolymers [11–23] and blending P(3HB) with suitable polymers are expected to improve its physical properties and make it the promising industrial polymeric materials in the near future [24–26].

Poly(3-hydroxybutyrate-*co*-3-hydroxyhexanoate) [P(3HB-*co*-3HHx)] is one of the promising bacterial P(3HB) copolymers, exhibiting significantly improved physical properties than those of P(3HB) due to its long side-chain [27–29]. So far, studies on the physical properties of P(3HB-*co*-3HHx) have been intensively described in several previous reports [28–35]. However, there are still some issues concerning on the hydrophobicity, low crystallization rate and high production cost of P(3HB-*co*-3HHx), and many efforts are being devoted to overcoming these limitations.

Polymer blending is one of the attractive and alternative choices to improve the polymeric materials into the desired physical properties. In our previous report [36], the miscibility, spherulite morphology, crystallization behavior and mechanical properties of P(3HB-*co*-3HHx)/poly (ethylene oxide) (PEO) binary blends has been described. It was found that the biocompatible, hydrophilic

* Corresponding author. Tel.: +81 45 924 5794; fax: +81 45 924 5827.
E-mail address: inoue.y.af@m.titech.ac.jp (Y. Inoue).

0032-3861/$ – see front matter © 2010 Elsevier Ltd. All rights reserved.
doi:10.1016/j.polymer.2010.09.042

and low production cost PEO played multiple roles as not only nucleating agent but also the plasticizer on improving several physical properties of hydrophobic and high production cost P(3HB-*co*-3HHx). Hence, PEO is taken as one of the very promising candidates of modifier on improving the physical properties of P(3HB-*co*-3HHx). Further detail studies are expected as the P(3HB-*co*-3HHx)/PEO binary blend is promising for medical applications due to their excellent biocompatibility and biodegradability.

Previous researches have characterized bacterially synthesized PHA copolymers, as mixtures or blends of random copolymers with different comonomer-unit compositional distribution. These copolymers can be comonomer-unit compositionally fractionated into a series of fractions with different comonomer-unit composition through a process of dissolution/precipitation by solvent/non-solvent mixed solvent [37,38]. It has also been demonstrated that this compositional distribution found in bacterial PHAs exhibits significant effect on their physical properties [39].

Therefore, in this work, the detail studies on P(3HB-*co*-3HHx)/PEO binary blend were conducted in order to reveal the effect of the unique feature of PHA copolymers, that is, the comonomer-unit composition and its distribution, on the miscibility and physical performance of P(3HB-*co*-3HHx)/PEO binary blends. The as-bacterially synthesized as well as well-fractionated P(3HB-*co*-3HHx)s with different 3HHx unit content were blended with PEO at different content. The physical performance including the thermal stability and mechanical properties of the P(3HB-*co*-3HHx)/PEO binary blends was estimated by thermogravimetric analysis and tensile test, respectively. The dispersion of PEO in the P(3HB-*co*-3HHx) matrix was characterized by scanning electron microscope. To our knowledge, this is the first report to reveal the effect of the comonomer-unit composition and its distribution of polyester on the miscibility of copolymer/homopolymer blending.

2. Experimental

2.1. Materials

As-bacterially synthesized P(3HB-*co*-3HHx) samples with 3HHx unit content of 7.5 mol-% ($M_w = 3.4 \times 10^5$, $M_w/M_n = 2.3$), 12.3 mol-% ($M_w = 2.2 \times 10^5$, $M_w/M_n = 3.7$), and 16.2 mol-% ($M_w = 1.1 \times 10^5$, $M_w/M_n = 2.8$), which were indicated as P(3HB-*co*-7.5 mol-% 3HHx), P(3HB-*co*-12.3 mol-% 3HHx) and P(3HB-*co*-16.2 mol-% 3HHx), respectively, were kindly supplied by Kaneka Corporation (Osaka, Japan) and were purified by precipitation in ethanol from chloroform solution. P(3HB-*co*-3HHx) with 3HHx unit content of 13.2 mol-% ($M_w = 4.3 \times 10^5$, $M_w/M_n = 2.3$), which was indicated as P(3HB-*co*-13.2 mol-% 3HHx), was biosynthesized by our group [31,32]. PEO sample was used as received ($M_v = 3.0 \times 10^5$ g mol^{-1}; Aldrich Chemical Co., Tokyo, Japan).

2.2. Fractionation

The as-bacterially synthesized P(3HB-*co*-3HHx) sample with 16.2 mol-% 3HHx unit content was comonomer-unit compositionally fractionated with a chloroform/*n*-heptane mixed solvent at ambient temperature according to the procedures previously applied for the fractionation of P(3HB-*co*-3HV) and P(3HB-*co*-3HP) as described elsewhere [16,17,31,32].

2.3. Preparation of P(3HB-co-3HHx)/PEO blends

The P(3HB-*co*-3HHx)/PEO blend films with desired PEO content were prepared by casting from chloroform solutions. The solvent was allowed to evaporate at room temperature overnight and then the resulted blend films were dried in a vacuum oven at 20 °C for at least one week to remove the residual solvents before any measurements.

2.4. Characterization of physical properties

2.4.1. Gel permeation chromatography (GPC)

Molecular weight of the samples was measured on TOSOH HLC-8220 GPC system (Tosoh Corporation, Tokyo, Japan) assembled with four TOSOH TSK GMH × 2 + 2000+1000HXL columns and a VISCOTEK T-60AV viscometer. Chloroform was used as an eluent at a flowing rate of 1.0 ml/min. The TOSOH TSK Standard polystyrene samples with narrow molecular distribution were used as standards to calibrate the GPC elution curve. The weight-average (M_w) molecular weight was calculated through a VISCOTEK TriSEC Data Acquisition System.

2.4.2. Differential scanning calorimetry (DSC)

DSC measurements were carried out to monitor the melting behavior on a Pyris Diamond DSC instrument (PerkinElmer Japan Co., Ltd., Yokohama, Japan). The scales of temperature and heat flow at different heating rates were calibrated using an indium standard with nitrogen purging.

The DSC heating and cooling scanning procedures were conducted as follows. About 3–5 mg sample was encapsulated in an aluminum pan and was held at −50 °C for 2 min, and then heated to 180 °C at a heating rate of 10 °C min^{-1}. After holding for 2 min at 180 °C to allow complete melting, the sample was cooled to −50 °C at a constant rate of −10 °C min^{-1}. Then after holding at −50 °C for 2 min, the sample was reheated to 180 °C at 10 °C min^{-1}.

2.4.3. ^{1}H NMR spectroscopy

Solution ^{1}H NMR spectra were recorded on a Bruker Ultrashield 600 MHz/54 mm NMR spectrometer (Bruker BioSpin AG, Fällanden, Switzerland) at room temperature. $CDCl_3$ and tetramethylsilane (TMS) were used as solvent and chemical shift reference, respectively. The assignments of the resonance peaks in the ^{1}H NMR spectra were in accordance with those previously reported [14].

2.4.4. Dynamic mechanical thermal analysis (DMTA)

DMTA was performed on a DMS210 (Seiko Instruments, Tokyo, Japan) equipped with a SSC5300 controller at a frequency of 1 Hz and a heating rate of 5 °C/min. The samples were thin rectangular strips with dimensions of about 30 × 10 × 0.15 mm^3.

2.4.5. FT-IR spectroscopy

Transmission FT-IR measurements were carried out on an AIM-8800 automatic infrared microscope (Shimadzu Co., Kyoto, Japan). The transmission FT-IR spectra were registered with an accumulation of 32 scans and a resolution of 2 cm^{-1} at room temperature. The film samples used for the FT-IR measurements were cast from chloroform solution.

2.4.6. Thermogravimetric analysis (TGA)

A TG/DTA 220 U with the Exstar 6000 Station (Seiko Instrument, Tokyo, Japan) was used for thermogravimetric analysis (TGA). The samples were scanned from 30 to 300 °C at a heating rate of 5 °C min^{-1} in the presence of nitrogen flow.

2.4.7. Tensile test

Mechanical properties were measured at room temperature using an EZ test machine (Shimadzu Corp., Kyoto, Japan). The gauge length and crosshead speed were 22.25 and 20 mm/min, respectively. The samples used for tensile test were prepared by film cast and the thickness of sample was ca. 0.15 mm.

2.4.8. Scanning electron microscopy (SEM)

The morphology of the surface of P(3HB-*co*-3HHx)/PEO blends with different PEO content were characterized by a scanning electron microscope model JSM-5200 (JEOL, Tokyo, Japan). The film samples used for SEM observation were put into acetone solvent for about 3 h to remove only the PEO component in order to elucidate the dispersion state of PEO in P(3HB-*co*-3HHx) film surface. Before the SEM surface characterization, the samples were coated under the coating currency of 6 mA for 2 min with the gold up to thickness of about 10 nm.

3. Results and discussion

3.1. Thermal behavior

DSC measurements are extensively applied for investigations of the miscibility of polymer blends. In the case of P(3HB-*co*-3HHx)/PEO binary blend, as the PEO shows a glass transition at a very low temperature range and also the increment of the heat capacity with its glass transition is not obvious enough to be observed by DSC, the DMTA is also applied to detect the glass transition temperature T_g of the blend system. Fig. 1(a) and (b) show the tan δ plotted against the temperature for the blends of P(3HB-*co*-7.5 mol-% 3HHx)/PEO and P(3HB-*co*-16.2 mol-% 3HHx)/PEO, respectively, with PEO content ranging from 0 to 60 wt.-%. To make a comparison, the results for pure P(3HB-*co*-7.5 mol-% 3HHx) and P(3HB-*co*-16.2 mol-% 3HHx) as well as PEO samples are also included.

According to Fig. 1(a) and (b), the T_g corresponding to P(3HB-*co*-3HHx) is obviously observed at around 10 and 0 °C for both the P(3HB-*co*-7.5 mol-% 3HHx)/PEO and P(3HB-*co*-16.2 mol-% 3HHx)/PEO blend systems, respectively, with the PEO content ranging from 0 to 30 wt.-%. While no T_g corresponding to PEO can be observed. With increasing the PEO content from 40 to 60 wt.-% in the blend, the T_g corresponding to both P(3HB-*co*-3HHx) and PEO can be observed. It shows that the blend has a single T_g when PEO content is less than 30 wt.-%, while double T_g appears when PEO weight composition is more than 40 wt.-%, indicating a sign of miscibility between both P(3HB-*co*-3HHx) samples and PEO when the PEO content is less than 30 wt.-%, and immiscibility when PEO content is more than 40 wt.-%. To further confirm the effect of the comonomer-unit composition of P(3HB-*co*-3HHx) on the miscibility between P(3HB-*co*-3HHx) and PEO, the DSC measurements were conducted.

Only one T_g can be observed for the respective blend samples during the range of DSC measurements. Fig. 2(a)–(d) show the T_g values measured by the DSC second heating scanning diagrams for

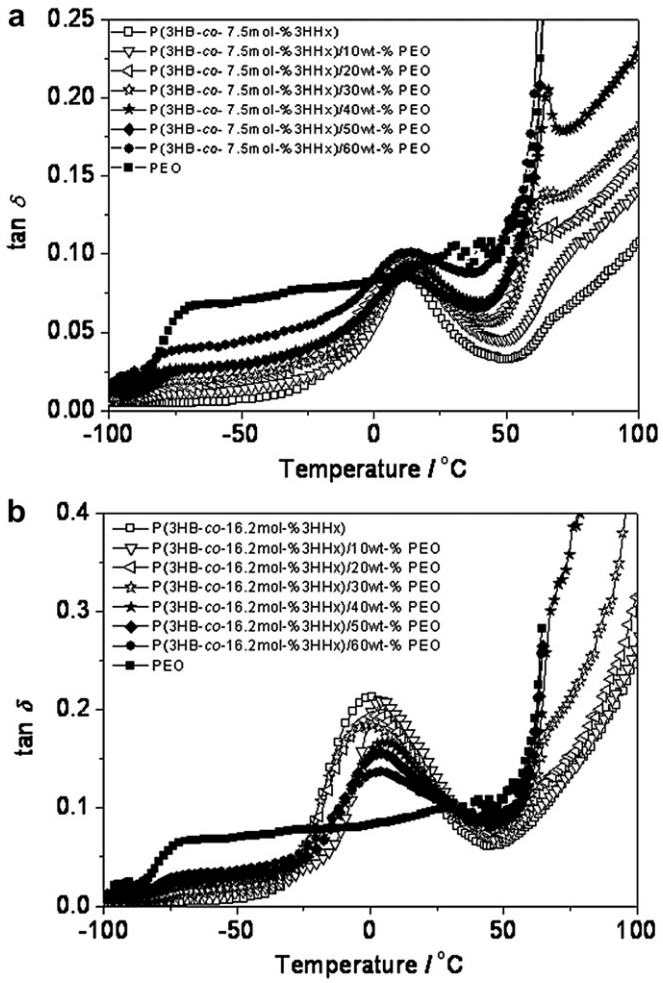

Fig. 1. The tan δ values plotted against the temperature for (a) P(3HB-*co*-7.5 mol-% 3HHx)/PEO (b) P(3HB-*co*-16.2 mol-% 3HHx)/PEO blends with different blend composition.

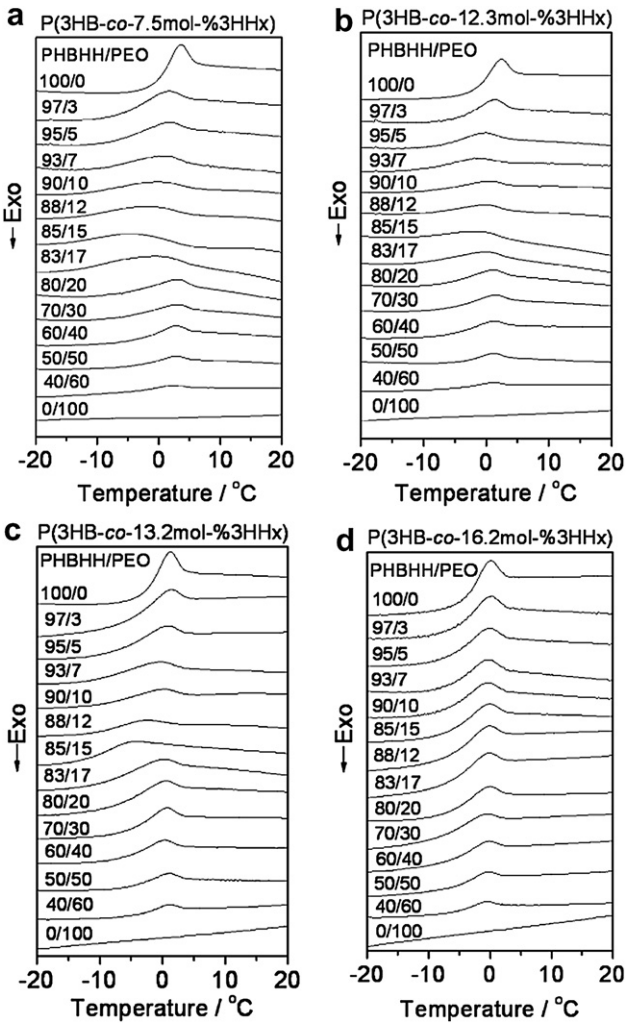

Fig. 2. The DSC thermograms of second heating scan (10 °C/min) of (a) P(3HB-*co*-7.5 mol-% 3HHx)/PEO, (b) P(3HB-*co*-12.3 mol-% 3HHx)/PEO, (c) P(3HB-*co*-13.2 mol-% 3HHx)/PEO and (d) P(3HB-*co*-16.2 mol-% 3HHx)/PEO blends with different blend composition. PHBHH indicates P(3HB-*co*-3HHx).

Table 1
T_g values of P(3HB-*co*-3HHx)/PEO blends with different blend composition.

PEO content/wt-%	T_g/°C			
	P(3HB-*co*-7.5 mol-% 3HHx)	P(3HB-*co*-12.3 mol-% 3HHx)	P(3HB-*co*-13.2 mol-% 3HHx)	P(3HB-*co*-16.2 mol-% 3HHx)
0	2.0	0.9	−0.2	−1.5
3	−1.1	−0.8	−0.6	−1.8
5	−2.3	−3.1	−2.2	−2.3
7	−3.3	−5.1	−4.5	−2.6
10	−7.0	−2.5	−4.0	−2.9
12	−7.4	−3.8	−5.9	−2.5
15	−10.5	−6.2	−7.9	−2.6
17	−7.8	−4.6	−4.0	−2.5
20	1.3	−1.6	−2.9	−2.5
30	1.5	−0.8	−1.1	−3
40	1.3	−0.9	−1.3	−2.1
50	1.2	−0.8	−0.9	−2
60	1.1	−0.8	−0.3	−1.9
100	−49.0	−49.0	−49.0	−49.0

P(3HB-*co*-7.5 mol-% 3HHx)/PEO, P(3HB-*co*-12.3 mol-% 3HHx)/PEO, P(3HB-*co*-13.2 mol-% 3HHx)/PEO and P(3HB-*co*-16.2 mol-% 3HHx)/PEO blends, respectively, with PEO content ranging from 0 to 100 wt.-%.

According to Fig. 2(a), it is observed that the T_g of P(3HB-*co*-7.5 mol-% 3HHx) decreases at first with increasing the PEO content to 17 wt.-%, then shifts to higher temperature and keeps almost the same for the blend samples with PEO content over 20 wt.-%. For the P(3HB-*co*-12.3 mol-% 3HHx)/PEO and P(3HB-*co*-13.2 mol-% 3HHx)/PEO blends as shown respectively in Fig. 2(b) and (c), the T_g of the blends similarly decreases at first with increasing the PEO content to 15 wt.-%, then shifts to higher temperature and keeps almost the same for the blend samples with PEO content over 20 wt.-%. For P(3HB-*co*-16.2 mol-% 3HHx)/PEO blends as shown in Fig. 2(d), the T_g of P(3HB-*co*-16.2 mol-% 3HHx) only decreases slightly for the blend sample with PEO content of 3 wt.-%, then keeps almost the same for the blend samples with PEO content of over 5 wt.-%.

The T_g values of the blends were further plotted as a function of blend composition, and the miscibility of the blends was further discussed by applying the Fox equation in order to predict the T_g dependence on the composition of the P(3HB-*co*-3HHx)/PEO blend. The Fox equation is represented as follows:

$$1/T_g^{blend} = W_a/T_g^a + W_b/T_g^b$$

where W_a and W_b are weight fraction of component polymers a and b, respectively. T_g^a and T_g^b represent the glass transition temperature of polymers a and b, respectively [40].

The T_g of P(3HB-*co*-3HHx) is summarized in Table 1, and Fig. 3 (a)–(d) show the T_g values plotted against the blend composition, in which the solid line indicates the T_g theoretically calculated from the Fox equation. The T_g values of the pure P(3HB-*co*-7.5 mol-% 3HHx), P(3HB-*co*-12.3 mol-% 3HHx), P(3HB-*co*-13.2 mol-% 3HHx) and P(3HB-*co*-16.2 mol-% 3HHx) as well as the pure PEO sample used in this study are 2.0, 0.9, −0.2, −1.5 and −49.0 °C, respectively.

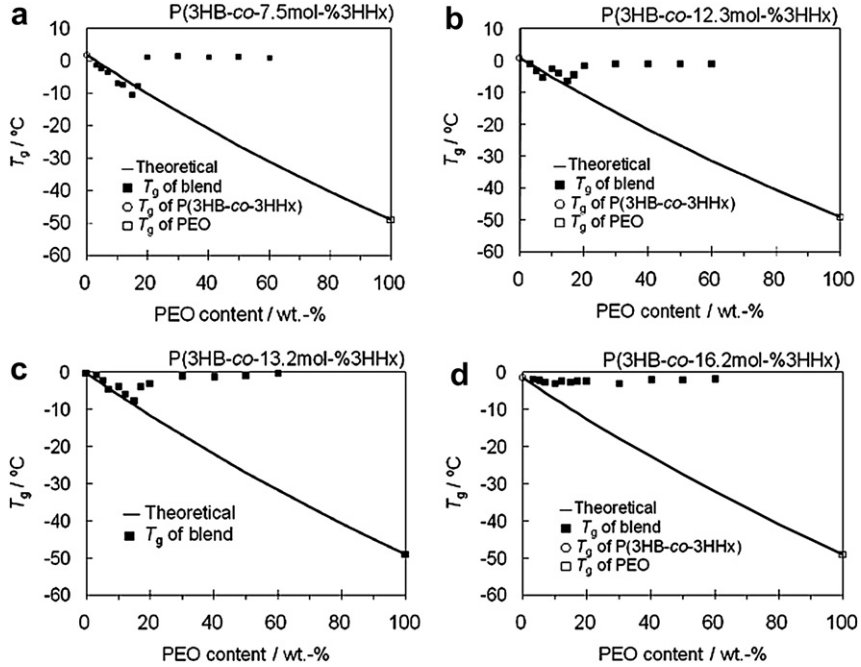

Fig. 3. Compositional dependence of glass transition temperature (T_g) for (a) P(3HB-*co*-7.5 mol-% 3HHx)/PEO, (b) P(3HB-*co*-12.3 mol-% 3HHx)/PEO, (c) P(3HB-*co*-13.2 mol-% 3HHx)/PEO and (d) P(3HB-*co*-16.2 mol-% 3HHx)/PEO blends. The solid line indicates the theoretical value calculated by the Fox equation.

As shown in Fig. 3(a), the T_g values of P(3HB-*co*-7.5 mol-% 3HHx)/PEO blend samples fit well with those calculated from the Fox equation with the PEO content increasing up to 17 wt.-%, while obvious deviation appears when the PEO content exceeds 20 wt.-%, indicating the blend samples with PEO content less than 17 wt.-% are miscible in the amorphous state, while the miscibility decreases dramatically when the PEO content exceeds 20 wt.-%. For P(3HB-*co*-12.3 mol-% 3HHx)/PEO and P(3HB-*co*-13.2 mol-% 3HHx)/PEO blend samples as shown in Fig. 3(b) and (c), the T_g values fit well with those calculated from the Fox equation with the PEO content increasing up to 15 wt.-%, and then show slight deviation with the PEO content of 17 wt.-%, while obvious deviation appears when the PEO content exceeding 20 wt.-%. For P(3HB-*co*-16.2 mol-% 3HHx)/PEO blend samples as shown in Fig. 3(d), however, the T_g values do not show obvious change with the PEO content, and deviate distinctly from those calculated from the Fox equation. This results indicate that the miscibility between P(3HB-*co*-3HHx) and PEO depends not only on the blend composition but also on the comonomer-unit composition of the P(3HB-*co*-3HHx) sample and it decreases dramatically with increasing both the PEO content in the blend and the 3HHx unit content of P(3HB-*co*-3HHx). It shows an indication that the 3HB component is miscible but the 3HHx component is not miscible with PEO.

To make it more obvious, the DSC first heating scanning diagrams for P(3HB-*co*-7.5 mol-% 3HHx) and P(3HB-*co*-16.2 mol-% 3HHx)/PEO blends are shown in Fig. 4(a) and (b), respectively.

According to Fig. 4(a), the melting peak corresponding to the PEO component of P(3HB-*co*-7.5 mol-% 3HHx)/PEO blend samples appears when the PEO content is 7 wt.-% and shifts to a lower temperature when that is 10 wt.-%, then shifts back to higher temperature when that is 20 wt.-%, indicating that PEO does not crystallize when the PEO content is less than 7 wt.-% in the blend and shows a good miscibility with P(3HB-*co*-7.5 mol-% 3HHx) when that is 10 wt.-%. While for P(3HB-*co*-16.2 mol-% 3HHx)/PEO blends as shown in Fig. 4(b), the melting peak corresponding to the PEO component appears only with 3 wt.-% PEO in the blend, and the peak position shifts slightly to a higher temperature with increasing the PEO content, indicating that PEO crystallizes in all blends and it shows almost no miscibility with P(3HB-*co*-16.2 mol-% 3HHx). This result further demonstrates that the 3HHx component is not miscible with PEO and the miscibility between P(3HB-*co*-3HHx) and PEO decreases dramatically with increasing both the 3HHx unit content of P(3HB-*co*-3HHx) and the PEO content in the blend. The immiscibility between 3HHx component and PEO is considered probably caused by the polarity, as PEO has polarity due to the

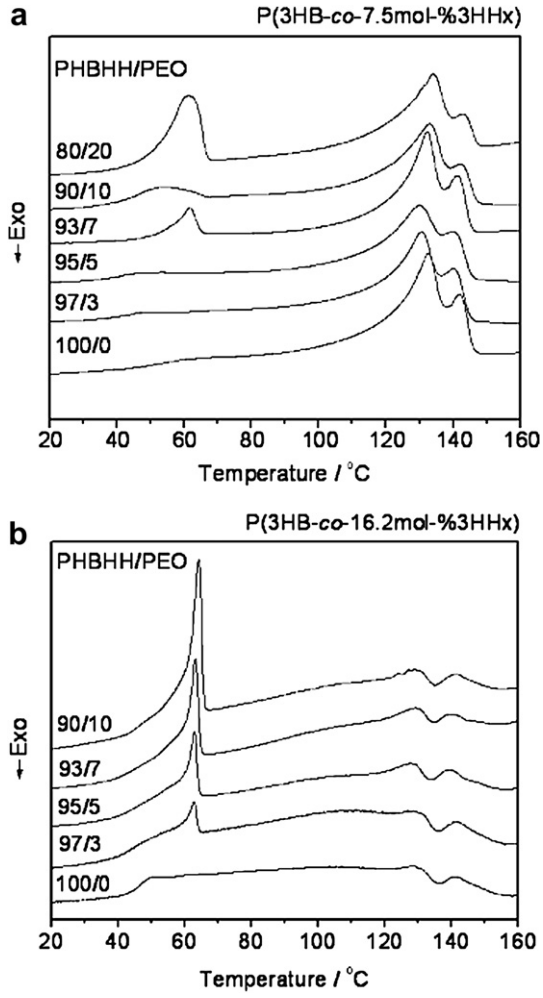

Fig. 4. The DSC thermograms of first heating scan (10 °C/min) of (a) P(3HB-*co*-7.5 mol-% 3HHx)/PEO blends with blend composition of 100/0, 97/3, 95/5, 93/7, 90/10, 80/20 and (b) P(3HB-*co*-16.2 mol-% 3HHx)/PEO blends with blend composition of 100/0, 97/3, 95/5, 93/7, 90/10. PHBHH indicates P(3HB-*co*-3HHx).

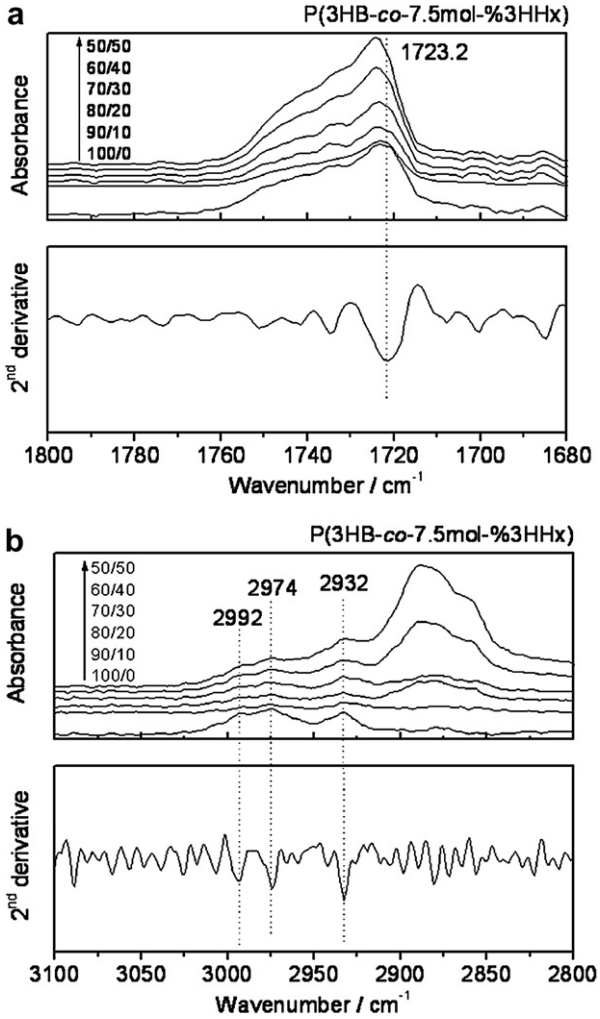

Fig. 5. FT-IR spectra of (a) carbonyl and (b) methyl absorption of P(3HB-*co*-3HHx) of P(3HB-*co*-7.5 mol-% 3HHx)/PEO blends with different blend composition at room temperature. The arrow indicates the P(3HB-*co*-3HHx)/PEO weight composition for each spectrum.

Table 2
Characterization of as-produced P(3HB-*co*-16.2 mol-% 3HHx) and its fractions.

Sample	Conc. of n-heptane (vol.-%)	Amount of sample in fraction (wt.-%)	3HHx[b] (%)	M_n[c] × 10^5	M_w[c] × 10^5	M_w/M_n[c]
P(3HB-*co*-16.2 mol-% 3HHx)[a]	–	100	16.2	0.4	1.1	2.8
Fraction 1	56.0	7.4	11.1	0.7	1.7	2.5
Fraction 2	58.0	5.9	8.9	0.5	1.4	2.5
Fraction 3	61.0	5.7	11.1	0.5	1.2	2.3
Fraction 4	64.0	9.4	13.2	0.4	1.2	3.0
Fraction 5	67.0	33.0	16.8	0.3	0.7	2.2
Fraction 6	70.0	17.8	20.4	0.2	0.4	1.9
Fraction 7	73.0	7.1	22.1	0.2	0.2	1.6
Fraction 8	73.0	0.3	19.2	0.1	0.2	1.7

[a] As-produced original sample.
[b] Measured by ^{1}H NMR.
[c] Measured by GPC.

existence of strong polar ether group, while the 3HHx unit almost doesn't have distinct polarity due to the existence of strong non-polar propyl group.

It is well known that the polymer–polymer miscibility usually involves hydrogen-bonding or other specific interactions between the components. In order to know the cause for the miscibility between PEO and P(3HB-*co*-3HHx) with low 3HHx unit content, the FT-IR measurement was conducted.

3.2. FT-IR analysis

FT-IR spectroscopy can provide information about molecular interactions, accordingly it has been intensively applied in detecting the existence of the hydrogen-bonding or other specific interactions in polymer–polymer blends. In the case of P(3HB-*co*-3HHx)/PEO blend, there are two possibilities to form hydrogen bonds between these two kinds of polymers. One is the hydrogen-bonding formed between the carbonyl group of P(3HB-*co*-3HHx) and the $-CH_2-$ group of PEO. The other is between the CH_3- group of P(3HB-*co*-3HHx) and the $-CH_2-O-CH_2-$ group of PEO.

The FT-IR spectra of the P(3HB-*co*-7.5 mol-% 3HHx)/PEO blend films with PEO content of 0–50 wt.-% cast from chloroform solution are shown in Fig. 5(a) and (b).

The absorption corresponding to the stretching of the carbonyl group of P(3HB-*co*-3HHx) appears at the range of 1700–1800 cm^{-1} as shown in Fig. 5(a). The second derivatives of the spectra are also included for confirmation and assignment of the peak corresponding to the absorption of the carbonyl group. According to Fig. 5(a), no obvious spectral change occurs with increasing the PEO content from 0 to 50 wt.-% in the blend, indicating the absence of hydrogen-bonding interaction between the carbonyl group of P(3HB-*co*-3HHx) and the $-CH_2-$ group of PEO.

Fig. 5(b) shows the absorption corresponding to the stretching of the CH_3- group of P(3HB-*co*-3HHx) in the range of 2800–3100 cm^{-1}. The second derivatives of the spectra are also included for confirmation and assignment of the peak corresponding to the absorption of the methyl group. Similarly, no obvious spectral change occurs with increasing the PEO content from 0 to 50 wt.-% in the blend, indicating no hydrogen-bonding formed between the CH_3- group of P(3HB-*co*-3HHx) and the $-CH_2-O-CH_2-$ group of PEO.

These demonstrate that the miscibility between P(3HB-*co*-3HHx) with high 3HB unit content and PEO is not caused by the formation of the hydrogen-bonding.

It is well known that P(3HB) is miscible with the PEO over the wide range of PEO content [26,41–43], and the as-bacterially synthesized P(3HB-*co*-3HHx) has a very broad comonomer-unit compositional distribution [31,32]. The above result also demonstrates that the 3HHx component is not miscible with PEO. Hence, it is reasonable to suggest that the miscibility between P(3HB-*co*-3HHx) with broad comonomer-unit compositional distribution and

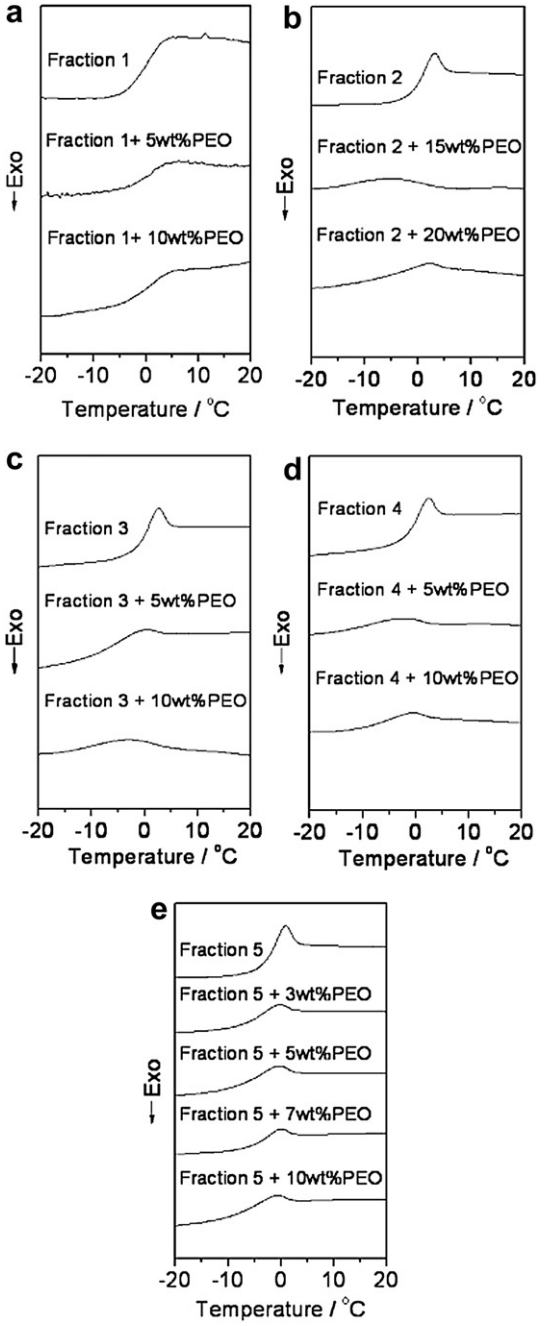

Fig. 6. The DSC thermograms of second heating scan (10 °C/min) of (a) Fraction 1/PEO, (b) Fraction 2/PEO, (c) Fraction 3/PEO, (d) Fraction 4/PEO and (e) Fraction 5/PEO blends with different blend composition.

PEO is caused by the miscibility between P(3HB-*co*-3HHx) component with high 3HB unit content and PEO, and the comonomer-unit composition and its distribution is suggested to play a key role in the miscibility between P(3HB-*co*-3HHx) and PEO. In order to investigate the effect of the comonomer-unit compositional distribution on the miscibility between P(3HB-*co*-3HHx) and PEO, the fractionation was conducted on the as-bacterially synthesized P(3HB-*co*-16.2 mol-% 3HHx) sample by the chloroform/*n*-heptane solvent/non-solvent mixture and the miscibility between the P(3HB-*co*-16.2 mol-% 3HHx) fractions with different 3HHx unit content and PEO were investigated.

3.3. Fractionation

The fractionation results of the as-bacterially synthesized P(3HB-*co*-16.2 mol-% 3HHx) are shown in Table 2.

According to Table 2, the original sample with 16.2 mol-% 3HHx unit content is fractionated into eight fractions with 3HHx unit content ranging from 8.9 to 22.1 mol-% and number-average molecular weight from 0.1×10^5 to 0.7×10^5. Except the Fraction 1, the 3HHx unit content of the fractions increases with fractionation proceeding from Fractions 2 to 7, and the molecular weight decreases from Fractions 1 to 8. It indicates that the fractionation of the as-bacterially synthesized P(3HB-*co*-16.2 mol-% 3HHx) depends on both 3HHx unit content and molecular weight.

3.4. Miscibility between the fractionated P(3HB-co-3HHx) and PEO

The miscibility between the Fractions 1 to 5 of the as-bacterially synthesized P(3HB-*co*-16.2 mol-% 3HHx) and PEO were investigated by the DSC measurements. Fig. 6(a)–(e) show the DSC second heating scanning diagrams for Fractions 1–5 blended with PEO, respectively.

The T_g values of the blends were further plotted as a function of blend composition as shown in Fig. 7(a)–(e).

According to Fig. 7(a), the T_g value of Fraction 1/PEO blend shows slight deviation from that calculated from the Fox equation when the PEO content in the blend is 5 wt.-%, while the deviation becomes significant when the PEO content in the blend increases to 10 wt.-%. On the other hand, for the Fraction 3, which has the similar 3HHx unit content to Fraction 1, the T_g values of the Fraction 3/PEO blends as shown in Fig. 7(c) fit well with those calculated from the Fox equation with the PEO content in the blend increasing up to 10 wt.-%.

For Fraction 5 with the 3HHx unit content of 16.8 mol-%, the T_g values of the Fraction 5/PEO blends as shown in Fig. 7(e) fit well with those calculated from the Fox equation when the PEO content

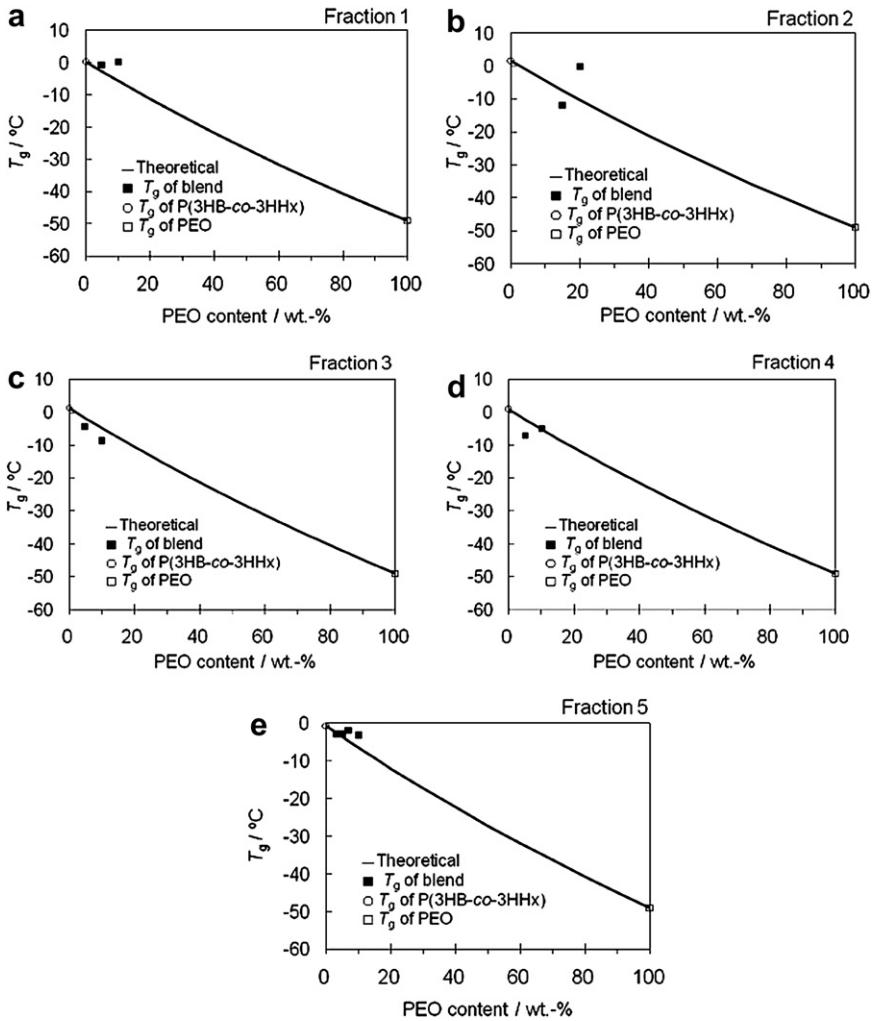

Fig. 7. Compositional dependence of glass transition temperature (T_g) for (a) Fraction 1/PEO, (b) Fraction 2/PEO, (c) Fraction 3/PEO, (d) Fraction 4/PEO and (e) Fraction 5/PEO blends. The solid line indicates the theoretical value calculated by the Fox equation.

in the blend is less than 7 wt.-%, while slight deviation appears when the PEO content exceeding 7 wt.-%. Compared the values for the Fraction 5/PEO blends to those for original sample with 16.2 mol-% 3HHx unit content, the T_g values of the original P(3HB-*co*-16.2 mol-% 3HHx)/PEO blends show obvious deviation from those calculated from the Fox equation when the PEO content in the blend is only 3 wt.-%. That is, there is obvious difference in the PEO content dependence of the T_g values between the Fraction 5/PEO and original P(3HB-*co*-16.2 mol-% 3HHx)/PEO blends, even this Fraction and the original sample have almost the same 3HHx unit content.

In the case of Fractions 1 and 3, as the 3HHx unit content of these two samples are the same, it is considered that their comonomer-unit compositional distribution are different because the first fraction of the fractionation of P(3HB-*co*-3HHx) usually still bears a relatively broad comonomer-unit compositional distribution [44]. In the case of the Fraction 5 with 16.8 mol-% 3HHx unit content and the original sample P(3HB-*co*-16.2 mol-% 3HHx), it is obvious that the original sample P(3HB-*co*-16.2 mol-% 3HHx) has a much broader comonomer-unit compositional distribution according to Table 2. This result reveals that the miscibility between P(3HB-*co*-3HHx) and PEO is not only affected by comonomer-unit composition but also significantly affected by the comonomer-unit compositional distribution of P(3HB-*co*-3HHx). The miscibility between P(3HB-*co*-3HHx) with broad comonomer-unit compositional distribution is caused by the miscibility between P(3HB-*co*-3HHx) component with high 3HB unit content and PEO. According to previous studies on P(3HB)/PEO blend, it is suggested there are some specific interactions between P(3HB) and PEO, as the P(3HB)-PEO interaction parameter is reported to be always negative, though it shows composition dependent [26]. While this specific interaction between P(3HB) and PEO is still not clear yet, further studies are expected.

3.5. Thermal stability

Our previous report has revealed that the crystallization and mechanical properties of P(3HB-*co*-3HHx) can be enhanced by blending with a certain weight content of PEO [36]. In the case of P(3HB-*co*-3HHx) with 11 mol-% 3HHx unit content, the crystallization of P(3HB-*co*-3HHx) can be accelerated by blending with 20–30 wt.-% PEO when the isothermal crystallization temperature is lower than the cold crystallization temperature of PEO, and the mechanical properties of P(3HB-*co*-3HHx) can be improved by blending with 5–17.5 wt.-% PEO.

The thermal stability of polymers is one of the fundamental properties that control their processability and applicability. In this work, thermogravimetric analysis (TGA) was applied to investigate whether the thermal stability of P(3HB-*co*-3HHx) can be improved by blending with PEO, as PEO is thermally stable compared to P(3HB-*co*-3HHx).

The TGA traces for P(3HB-*co*-7.5 mol-% 3HHx) and P(3HB-*co*-16.2 mol-% 3HHx)/PEO blends with PEO content of 0, 10, 20 and 30 wt.-% are shown respectively in Fig. 8(a) and (b).

It can be seen that all the investigated samples exhibit an one-step weight loss mechanism which is ascribed to P(3HB-*co*-3HHx), while PEO does not show thermal decomposition at the temperature lower than 300 °C under nitrogen atmosphere. It can also be observed that the TGA curves shifted towards lower temperature range with increasing the PEO content for P(3HB-*co*-7.5 mol-% 3HHx). While for P(3HB-*co*-16.2 mol-% 3HHx)/PEO blend, the TGA curves shifted towards high temperature range by blending with PEO of less than 30 wt.-%.

The temperatures at 5% decomposition weight loss, indicated as $T_{d(5\%)}$, are listed in Table 3.

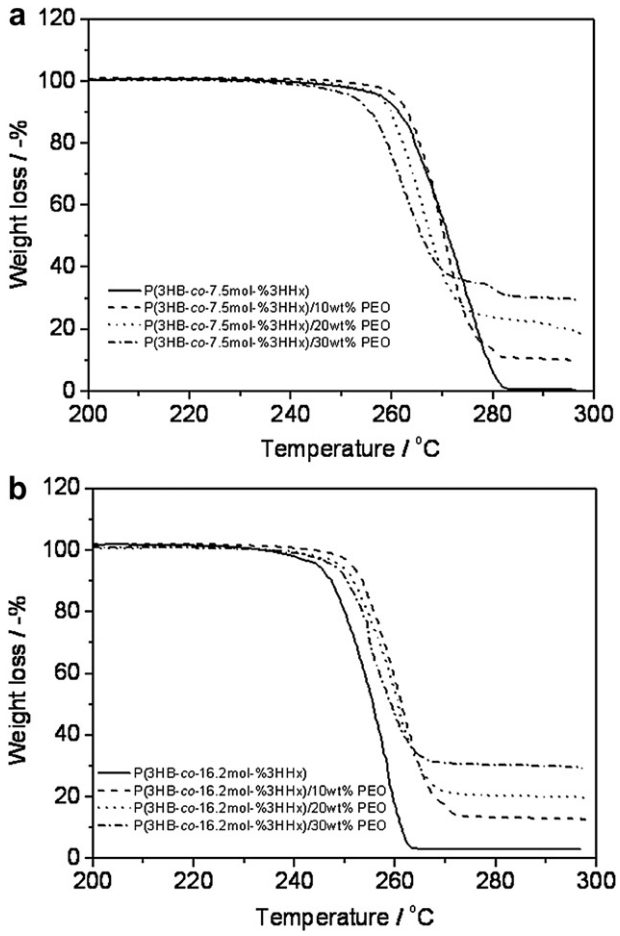

Fig. 8. TGA weight loss curves for (a) P(3HB-*co*-7.5 mol-% 3HHx)/PEO (b) P(3HB-*co*-16.2 mol-% 3HHx)/PEO blends with different blend composition.

According to Table 3, the $T_{d(5\%)}$ decreases with increasing the PEO content from 0 to 30 wt.-% for P(3HB-*co*-7.5 mol-% 3HHx)/PEO blend. While for P(3HB-*co*-16.2 mol-% 3HHx)/PEO blend, the $T_{d(5\%)}$ firstly increases with increasing the PEO content to 10 wt.-%, then decreases with increasing the PEO content to 30 wt.-%. It indicates that the thermal stability of P(3HB-*co*-7.5 mol-% 3HHx) is deteriorated by blending with PEO. For P(3HB-*co*-16.2 mol-% 3HHx), however, the thermal stability can be enhanced by blending with PEO, though the enhancement effect is depending on the PEO content in the blend.

It is widely believed that the thermal degradation of PHAs occurs almost exclusively by a non-radical random chain–scission reaction [45–49]. The thermal decomposition mechanism consists of a gradual decrease in the molecular weight. It is considered that the presence of the 3HHx unit in the P(3HB) polymer chain probably leads to a faster degradation since the propyl group possesses

Table 3
$T_{d(5\%)}$ of P(3HB-*co*-3HHx)/PEO blends with different blend composition.

PEO content/wt.-%	$T_{d(5\%)}$/°C	
	P(3HB-*co*-7.5 mol-% 3HHx)	P(3HB-*co*-16.2 mol-% 3HHx)
0	267	245
10	260	252
20	257	249
30	248	248

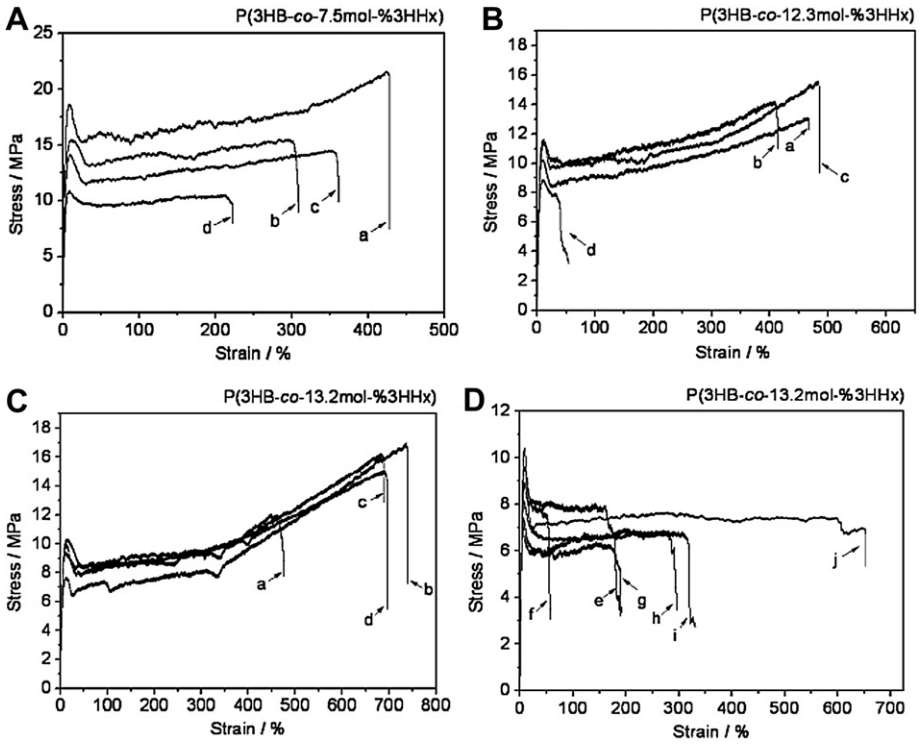

Fig. 9. Stress–strain curves of (A) (a) pure P(3HB-*co*-7.5 mol-% 3HHx) and its blends with PEO of (b) 10 wt.-%, (c) 20 wt.-%, (d) 30 wt.-%; (B) (a) pure P(3HB-*co*-12.3 mol-% 3HHx) and its blends with PEO of (b) 10 wt.-%, (c) 20 wt.-%, (d) 30 wt.-%; (C) (a) pure P(3HB-*co*-13.2 mol-% 3HHx) and its blends with PEO at (b) 10 wt.-%, (c) 20 wt.-%, (d) 30 wt.-% (D) P(3HB-*co*-13.2 mol-% 3HHx) blends with PEO of (e) 40 wt.-%, (f) 50 wt.-%, (g) 60 wt.-%, (h) 70 wt.-%, (i) 80 wt.-% and (j) pure PEO.

a stronger electron-donating effect than the methyl one [50]. This stronger electron-releasing effect of the propyl group might enhance the formation of the alkenyl end group, as it stabilizes the sp^2 carbon atoms of the double bond more than the methyl would [50]. Moreover, P(3HB-*co*-7.5 mol-% 3HHx) has a higher molecular weight than P(3HB-*co*-16.2 mol-% 3HHx). Therefore, the thermal stability of P(3HB-*co*-7.5 mol-% 3HHx) is higher than that of P(3HB-*co*-16.2 mol-% 3HHx).

By blending with PEO, in the case of P(3HB-*co*-7.5 mol-% 3HHx), the presence of PEO with a low content may probably lead to a faster degradation as PEO is miscible with P(3HB-*co*-3HHx) in this case and the interactions between PEO and P(3HB-*co*-3HHx) component with high 3HB unit content probably accelerate the random chain–scission reaction of P(3HB-*co*-3HHx) polymer chain. While in the case of P(3HB-*co*-16.2 mol-% 3HHx), as the blend system is not miscible, the presence of PEO with a low content may probably act as a decomposition-retardant which hinders the thermal mobility of P(3HB-*co*-3HHx) polymer chain resulting in an improved thermal stability. With increasing the PEO content in the blend, the significant phase separation and the decrease of P(3HB-*co*-3HHx) domain is considered to be the cause of a faster thermal degradation.

These TGA results indicate that the blending with PEO can exhibit different effect on the thermal stability of P(3HB-*co*-3HHx), which is not only depending on the PEO content in the blend but also on the comonomer-unit composition of P(3HB-*co*-3HHx).

Table 4
Mechanical properties of P(3HB-*co*-3HHx)/PEO blend samples.

Sample	PEO content/%	Young's modulus/MPa	Yield strength/MPa	Elongation at break/%
P(3HB-*co*-7.5 mol-% 3HHx)	0	253.2 ± 59.0	20.2 ± 2.2	435.8 ± 24.7
	10	0.6 ± 0.0	15.9 ± 0.8	336.7 ± 21.7
	20	0.7 ± 0.0	15.3 ± 1.1	356.3 ± 9.9
	30	9.2 ± 0.0	11.6 ± 0.6	252.8 ± 6.2
P(3HB-*co*-12.3 mol-% 3HHx)	0	6.5 ± 2.9	15.7 ± 1.8	445.4 ± 25.7
	10	3.9 ± 1.4	14.9 ± 2.1	410.1 ± 31.2
	20	5.3 ± 1.3	13.1 ± 0.3	456.1 ± 26.7
	30	7.0 ± 0.1	8.9 ± 0.4	67.7 ± 4.2
P(3HB-*co*-13.2 mol-% 3HHx)	0	3.3 ± 0.4	11.2 ± 1.5	457.9 ± 37.6
	10	1.4 ± 0.0	19.2 ± 3.2	759.1 ± 37.6
	20	5.2 ± 0.0	16.2 ± 0.0	689.7 ± 10.0
	30	2.0 ± 0.8	14.4 ± 0.9	710.7 ± 19.5
	40	6.3 ± 0.4	8.8 ± 0.1	173.5 ± 21.6
	50	3.4 ± 3.4	9.3 ± 0.4	55.3 ± 4.9
	60	5.8 ± 0.3	8.1 ± 0.7	178.5 ± 7.2
	70	5.4 ± 1.7 ($\times 10^{-2}$)	7.9 ± 0.7	295.0 ± 12.9
	80	4.6 ± 1.4 ($\times 10^{-2}$)	7.9 ± 0.4	331.1 ± 9.5
	100	192.1 ± 13.6	16.0 ± 2.4	783.5 ± 85.6

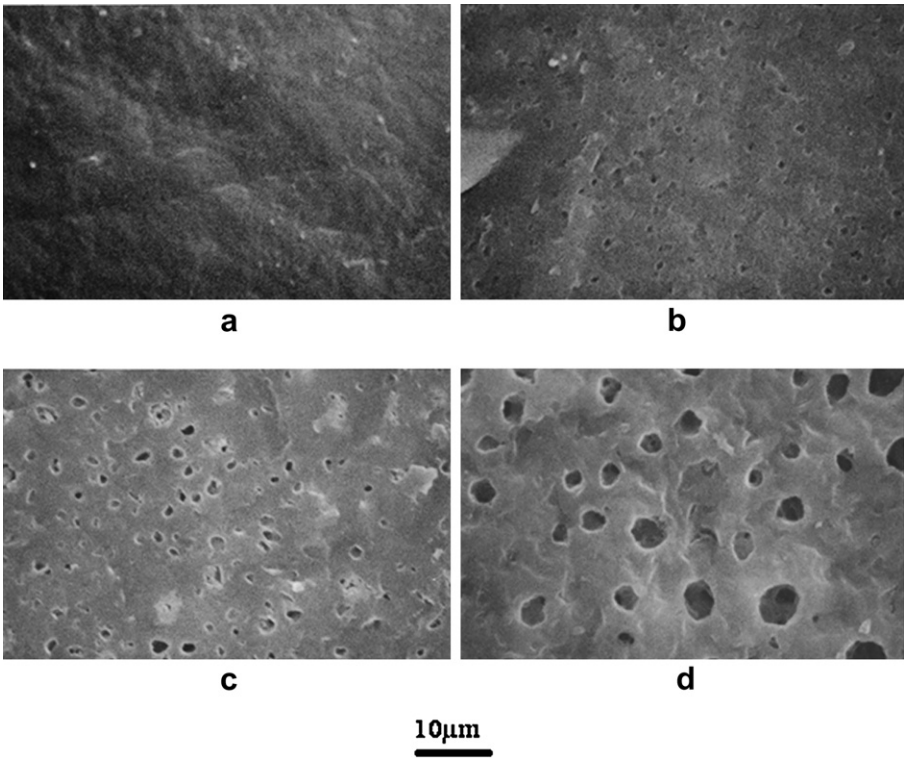

Fig. 10. SEM photographs for (a) pure P(3HB-*co*-7.5 mol-% 3HHx) and P(3HB-*co*-7.5 mol-% 3HHx)/PEO blends with PEO weight fraction of (b) 5 wt.-%, (c) 10 wt.-% (d) 20 wt.-%, scale bar for (a) – (d): 10 μm.

3.6. Mechanical properties

In order to know how the comonomer-unit composition of P(3HB-*co*-3HHx) and the miscibility between P(3HB-*co*-3HHx) and PEO affect the mechanical performance of the P(3HB-*co*-3HHx)/PEO binary blend material, the tensile test were conducted.

The stress-strain curves of P(3HB-*co*-7.5 mol-% 3HHx)/PEO, P(3HB-*co*-12.3 mol-% 3HHx)/PEO and P(3HB-*co*-13.2 mol-% 3HHx)/PEO blends with different blend composition are shown in Fig. 9 and the mechanical data are summarized in Table 4.

In the case of P(3HB-*co*-7.5 mol-% 3HHx), the elongation at break decreases with increasing the PEO content to 10 wt.-%, then increases slightly when the PEO content is 20 wt.-%, while decreases significantly with the PEO content increasing to 30 wt.-%. The Young's modulus, however, decreases significantly when the PEO content increasing to 10 wt.-% and then increases with increasing PEO content to 30 wt.-%. In general, the yield strength decreases with increasing the PEO content. It indicates that the miscibility between PEO and P(3HB-*co*-3HHx) with low 3HHx unit content leads to a significant deterioration in the modulus of the blend sample and a slight decrease in the elongation at break.

For P(3HB-*co*-12.3 mol-% 3HHx), the elongation at break similarly decreases by blending with 10 wt.-% PEO, then increases with further increasing the PEO content to 20 wt.-%, while decreases dramatically with the PEO content increasing to 30 wt.-%. Though not as significant as in the case of P(3HB-*co*-7.5 mol-% 3HHx), the Young's modulus decreases with increasing the PEO content to 10 wt.-% and then increases with increasing to 30 wt.-%, where the Young's modulus of the blend sample is a little higher than that of the pure sample. The yield strength similarly decreases with increasing the PEO content.

In the case of P(3HB-*co*-13.2 mol-% 3HHx), the elongation at break is significantly enhanced by blending with 10 wt.-% PEO, while it decreases with increasing the PEO content to 50 wt.-%, then increases again by further increasing the PEO content to 100 wt.-%. Similar to previous two P(3HB-*co*-3HHx) samples, the Young's modulus of blend samples decreases with increasing the PEO content to 10 wt.-% then increases with further increasing the PEO content, while it decreases significantly when the PEO content is over 70 wt.-% in the blend. The yield strength is in general decreases with increasing the PEO content in the blend, while different to the previous cases, the yield strength of blend samples with the PEO content less than 30 wt.-% is improved compared to the pure sample. It indicates that the miscibility between PEO with content less than 30 wt.-% and P(3HB-*co*-3HHx) with higher 3HHx unit content can enhance the elongation at break, though it leads to a slight decrease in the modulus.

It is considered that a low content of PEO in the blend acts as diluents in the amorphous phase of P(3HB-*co*-3HHx) with higher 3HHx unit content, as PEO is miscible with P(3HB-*co*-3HHx) and accordingly can enter the amorphous phase of P(3HB-*co*-3HHx). However, in the case of P(3HB-*co*-3HHx) with lower 3HHx unit content, though a low content of PEO can enter the amorphous phase of P(3HB-*co*-3HHx) due to the miscibility, while the role of PEO as a diluent is less obvious as the interactions between PEO and P(3HB-*co*-3HHx) component with high 3HB content are stronger due to the low 3HHx unit content of P(3HB-*co*-3HHx), leading to a hindering effect on the mobility of P(3HB-*co*-3HHx) polymer chain and accordingly resulting in a decrease in the elongation at break.

The above results demonstrate that the miscibility between P(3HB-*co*-3HHx) and PEO is a requirement to an improved mechanical performance of P(3HB-*co*-3HHx)/PEO blend, while this

improvement effect depends significantly on the comonomer-unit composition of P(3HB-*co*-3HHx).

3.7. Scanning electron microscopy (SEM)

The surface morphology of pure P(3HB-*co*-7.5 mol-% 3HHx) and P (3HB-*co*-7.5 mol-% 3HHx)/PEO blend films with the PEO content of 5, 10 and 20 wt.-% were characterized by SEM. In order to investigate the dispersion of PEO in P(3HB-*co*-3HHx) matrix, the investigated films were processed by dipping in acetone for 3 h to remove the PEO component in the blend. The SEM photographs are shown in Fig. 10 (a)–(d).

It is clearly shown that a porous surface of P(3HB-*co*-3HHx) film can be formed by blending with PEO. In the case of the blend with 5 wt.-% PEO, the average diameter of the pore is around 1 μm. With increasing the PEO content to 10 wt.-%, the average diameter of the pore increases to about 2 μm, and it further increases to 5 μm with increasing the PEO content to 20 wt.-% in the blend. This result indicates that the diameter of the porous morphology linearly expands with increasing the PEO content in the blend. By varying the weight content of PEO in the blend, it is able to regulate the porous morphology. It is also shown that PEO exhibits a good dispersion in P(3HB-*co*-3HHx) matrix. This result reveals that the P (3HB-*co*-3HHx)/PEO blend is promising for the fabrication of porous materials for medical applications due to the excellent biocompatibility and biodegradability of this blend.

4. Conclusions

The as-bacterially synthesized P(3HB-*co*-3HHx) samples with 7.5, 12.3, 13.2 and 16.2 mol-% 3HHx unit content were used to investigate the effect of the comonomer-unit composition of P (3HB-*co*-3HHx) on the miscibility of P(3HB-*co*-3HHx)/PEO blends. It is found that the miscibility between P(3HB-*co*-3HHx) and PEO decreases dramatically with increasing both the 3HHx unit content of P(3HB-*co*-3HHx) and the PEO content in the blend. By conducting the fractionation on the as-bacterially synthesized P (3HB-*co*-3HHx) sample with 16.2 mol-% 3HHx unit content, it is found that the miscibility between P(3HB-*co*-3HHx) and PEO is significantly affected by the comonomer-unit compositional distribution of P(3HB-*co*-3HHx). It is suggested that the miscibility between P(3HB-*co*-3HHx) with broad comonomer-unit compositional distribution and PEO is caused by the miscibility between PEO and P(3HB-*co*-3HHx) component with high 3HB unit content. Depending on both the comonomer-unit composition of P(3HB-*co*-3HHx) and the blend composition, PEO exhibits different effect on the thermal stability and mechanical performance of P(3HB-*co*-3HHx). By SEM characterization, PEO is found to exhibit good dispersion in P(3HB-*co*-3HHx). It is concluded that the P(3HB-co-3HHx)/PEO binary blend can exhibit diverse properties by varying the comonomer-unit composition and comonomer-unit compositional distribution of P(3HB-*co*-3HHx) and also the PEO content in the blend, which is promising for numerous applications in particular the medical applications. Future work is expected on explanation of specific interactions between P(3HB) and PEO as well as the regulation of biodegradability of P(3HB-*co*-3HHx) by blending with PEO.

References

[1] Anderson AJ, Dawes EA. Microbiol Rev 1990;54:450–72.
[2] Steinbüchel A. Curr Opin Biotechnol 1992;3:291–7.
[3] Lee SY, Chang HN. Adv Biochem Eng Biotechnol 1995;52:27–58.
[4] Steinbüchel A, Valentin HE. FEMS Microbiol Lett 1995;128:219–28.
[5] Steinbüchel A, Füchtenbusch B. Trends Biotechnol 1998;16:419–27.
[6] Sudesh K, Abe H, Doi Y. Prog Polym Sci 2000;25:1503–55.
[7] Lemoigne M. Bull Soc Chim Biol 1926;8:770–82.
[8] Howells ER. Chem Ind 1982;8:508–11.
[9] King PP. Chem Technol Biotechnol 1982;32:2–8.
[10] Holmes PA. Phys Technol 1985;16:32–6.
[11] Bloembergen S, Holden DA, Hamer GK, Bluhm TL, Marchessault RL. Macromolecules 1986;19:2865–71.
[12] Kunioka N, Tamaki A, Doi Y. Macromolecules 1989;22:694–7.
[13] Kamiya N, Yamamoto Y, Inoue Y, Chûjô R. Macromolecules 1989;22:1676–82.
[14] Doi Y, Kunioka M, Nakamura Y, Soga K. Macromolecules 1986;19:2860–4.
[15] Yoshie N, Menju H, Sato H, Inoue Y. Macromolecules 1995;28:6516–21.
[16] Cao A, Ichikawa M, Kasuya K, Yoshie N, Asakawa N, Inoue Y, et al. Polym J 1996;28:1096–102.
[17] Cao A, Kasuya K, Abe H, Doi Y, Inoue Y. Polymer 1998;39:4801–16.
[18] Arai Y, Cao A, Yoshie N, Inoue Y. Polym Int 1999;48:1219–28.
[19] Wang Y, Ichikawa M, Cao A, Yoshie N, Inoue Y. Macromol Chem Phys 1999;200:1047–53.
[20] Cao A, Asakawa N, Yoshie N, Inoue Y. Polymer 1999;40:3309–22.
[21] Doi Y, Segawa A, Kunioka M. Int J Biol Macromol 1990;12:106–11.
[22] Saito Y, Doi Y. Int J Biol Macromol 1994;16:99–104.
[23] Shi F, Ashby RD, Gross RA. Macromolecules 1997;30:2521–3.
[24] Yang XS, Zhao K, Chen G-Q. Biomaterials 2002;23:1391–7.
[25] Zhao K, Deng Y, Chen JC, Chen G-Q. Biomaterials 2003;24:1041–5.
[26] Avella M, Martuscelli E. Polymer 1988;29:1731–7.
[27] Shiotani T, Kobayashi G. Japanese Pat Appl 93049; 1993.
[28] Shimamura E, Kasuya K, Kobayashi G, Shiotani T, Shima Y, Doi Y. Macromolecules 1994;27:878–80.
[29] Doi Y, Kitamura S, Abe H. Macromolecules 1995;28:4822–8.
[30] Kichise T, Fukui T, Yoshida Y, Doi Y. Int J Biol Macromol 1999;25:69–77.
[31] Watanabe T, He Y, Fukuchi T, Inoue Y. Macromol Biosci 2001;1:75–83.
[32] Feng L, Watanabe T, Wang Y, Kichise T, Fukuchi T, Chen G-Q, et al. Biomacromolecules 2002;3:1071–7.
[33] Wang YW, Wu Q, Chen G-Q. Biomaterials 2004;25:669–75.
[34] Wang YW, Wu Q, Chen G-Q. Biomaterials 2005;26:899–904.
[35] Wang YW, Mo W, Yao H, Wu Q, Chen JC, Chen G-Q. Polym Degrad Stabil 2004;85:815–21.
[36] Yu F, Nakayama T, Nakamura N, Katsumata K, Pan P, Inoue Y. Macromol Mater Eng 2009;294:868–76.
[37] Yoshie N, Inoue Y. Int J Biol Macromol 1999;25:193–200.
[38] Feng L, Yoshie N, Asakawa N, Inoue Y. Macromol Biosci 2004;4:186–98.
[39] Yu F, Zhu B, Dong T, Inoue Y. Macromol Biosci 2009;9:702–12.
[40] Fox TG. Bull Am Phys Soc 1956;1:123–35.
[41] Reeve MS, McCarthy SP, Gross RA. Macromolecules 1993;26:888–94.
[42] Na YH, He Y, Asakawa N, Yoshie N, Inoue Y. Macromolecules 2002;35:727–35.
[43] Chee MJK, Ismail J, Kummerlöwe C, Kammer HW. Polymer 2002;43:1235–9.
[44] Yu F, Nakamura N, Inoue Y. Polymer 2010;51:4408–18.
[45] Carothers WH. J Am Chem Soc 1932;54:4066–70.
[46] Grassie N, Murray EJ, Holmes PA. Polym Degrad Stab 1984;6:47–61.
[47] Grassie N, Murray EJ, Holmes PA. Polym Degrad Stab 1984;6:95–103.
[48] Lehrle RS, Williams RJ. Macromolecules 1994;27:3782–9.
[49] Abate R, Ballistreri A, Montaudo G. Macromolecules 1994;27:332–6.
[50] Nguyen S, Yu G, Marchessault RH. Macromolecules 2002;3:219–24.